Noname manuscript No.
(will be inserted by the editor)

Quasi-Wollaston-prism for terahertz frequencies fabricated by 3D printing

A.I. Hernandez-Serrano · E. Castro-Camus

Received: date / Accepted: date

Abstract In this letter we present the design, fabrication and characterization of a quasi-Wollaston prism for terahertz frequencies based on form birrefringence. The prism uses the birrefringence induced in a sub-wavelength layered plastic-air structure that produces refraction in different directions for different polarizations. The component was simulated using the finite-difference-time-domain method, fabricated by 3D printing and subsequently tested by terahertz time-domain spectroscopy showing a polarization separation around of 23° for frequencies below 400 GHz, exhibiting cross polarization power extinction ratios better than 1.6×10^{-3} at 200 GHz.

Keywords Wollaston prism · Form birrefringence · Effective-medium-theory

Terahertz radiation has become a powerful tool for a number of scientific and real-world applications that include security [1–3], industrial inspection [4–6], cultural heritage evaluation [7,8], semiconductor characterization [9], wireless communications [10–12] among many others. Therefore devices to manipulate radiation in this spectral band are in growing demand. Unfortunately many materials, transparent in the visible range, are opaque at terahertz frequencies. Previous studies demonstrate that many 3D-printable polymers are transparent at terahertz frequencies [13]. Three dimensional printing has gained attention owing to its capability of rapidly producing prototypes of objects with complex geometries that can easily be computer designed. Furthermore, users of this technology can easily produce programs in order to directly control the motion of the printer which allows them using the full capacity for the production of components with resolution-limited features [16]. Typically the resolution of a fused-polymer-injection printer is around 400 μm. This res-

Centro de Investigaciones en Optica A.C., Loma del Bosque 115, Lomas del Campestre, Leon, Guanajuato 37150, Mexico
Tel.: +52 (477) 441-42-00
Fax: +52 (477) 441-42-09
E-mail: enrique@cio.com

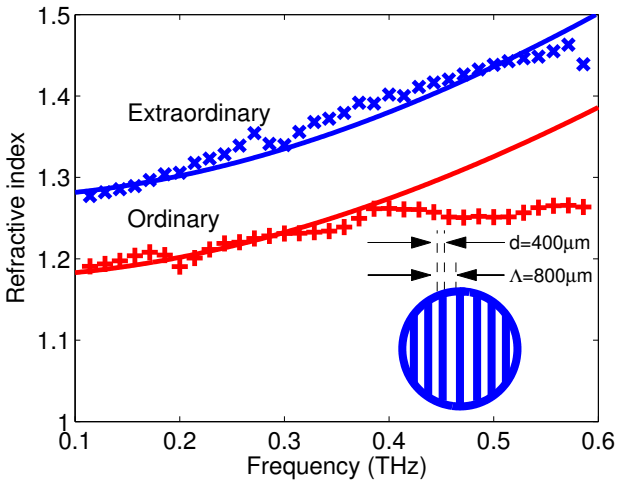

Fig. 1 Ordinary (perpendicular to the layers) and extraordinary (parallel to the layers) refractive indices of the birrefringent structure. The continuous lines are the predicted refractive index for the two orthogonal orientations and the circle and squares are experimental measurements. The curves agree for frequencies below 400 GHz. Inset shows the form-birrefringent structure used for this characterization.

olution was proven to be good enough to make THz devices appropriate for frequencies below ~ 800 GHz. Examples are, lenses and gratings [13–15], terahertz optical fibers [17,18], grin lenses [16,19], zone plates [20] and waveguides [21–24]. In this article we use 3D printing in order to make a polarization splitter, similar to a Wollaston prism, using form birrefringence [25]. Firstly the design was modeled using a finite-difference-time-domain simulation [26]. The device was printed and subsequently tested using a terahertz time-domain spectroscopy system. The experiments demonstrated apolarization around 30° for frequencies below 400 GHz.

In order to make the polarization splitter we induce form birefringence by building a layered structure that combines air and Bendlay. The device was fabricated using a Prusa i3 printer with a 400μm nozzle which determines its resolution. Firstly we made a sample with $d = 400\,\mu$m-thick walls of Bendlay (n=1.53 below 1 THz) with period of $\Lambda = 800\,\mu$m [13]. This structure is schematically shown in the inset of Fig. 1. The solid lines in Fig. 1 are the predicted refractive indices for such structure [25], given by

$$n_e^2 = n_\parallel^2 + \frac{1}{3}\left[\frac{\Lambda}{\lambda}\pi f_1 f_2 (n_1^2 - n_2^2)\right]^2 \tag{1}$$

and

$$n_o^2 = n_\perp^2 + \frac{1}{3}\left[\frac{\Lambda}{\lambda}\pi f_1 f_2 \left(\frac{1}{n_1^2} - \frac{1}{n_2^2}\right) n_\parallel n_\perp^3\right]^2 \tag{2}$$

where Λ is the structure period, λ is the wavelength, $n_1 = 1.53$ and $n_2 = 1$ are the refractive indices of the layers, f_1 and f_2 are their respective volumetric

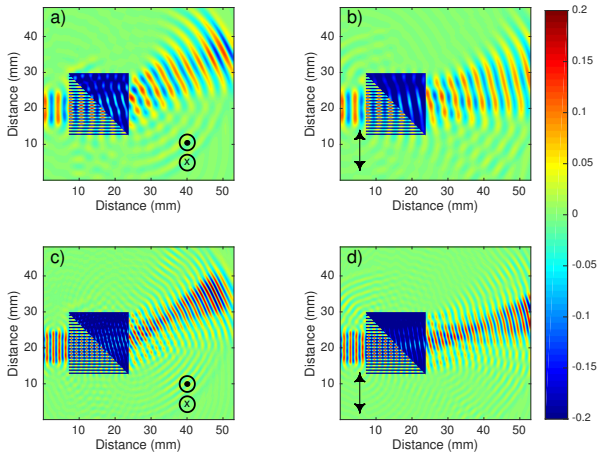

Fig. 2 Electric field calculated by finite-difference-time-domain simulation for the device proposed. The Wollaston prism was made of 400 μm spacing n=1.0 and parallel walls n=1.53, valid below 1 THz, in a triangular configuration and a solid prism of the same material. a) and b) show simulation results for polarizations parallel and perpendicular to the layers respectively with an incident plane wave at 100 GHz. c) and d) show the analogous simulations to a) and b) at 600 GHz. The deflected angles are approximately 29° and 11° for the polarization parallel and perpendicular respectively

fractions,

$$n_{\parallel}^2 = f_1 n_1^2 + f_2 n_2^2 \tag{3}$$

and

$$n_{\perp}^2 = \left(\frac{f_1}{n_1^2} + \frac{f_2}{n_2^2} \right)^{-1} . \tag{4}$$

The two refractive indices of the material were measured using terahertz time-domain spectroscopy with linearly polarized pulses parallel and perpendicuilar to the material layers of the sample and the analysis was perform as described in [25]. The crosses and squares in Fig. 1 are the experimentally measured refractive indices for the ordinary and extraordinary polarizations. The measurements are in acceptable agreement with the theoretical predictions for frequencies below 400 GHz. The discrepancy for higher frequencies can be attributed to the fact that higher frequencies (shorter wavelengths) are comparable or shorter to the features of the structure, which in turn produces diffraction and guiding in the layers, which are highly anisotropic and are not considered in the model used for the solid lines.

The geometry we propose for the quasi-Wollaston prism is schematically shown in Fig. 3a. This component is a cubic object with a layered structure in one half of it, similar to the one used for the form birefringence characterization, and solid material in the other half. The two halves meet at a 45° angle forming a component similar to a Wollaston prism. We simulated such structure using a finite-difference-time-domain model. The results for the

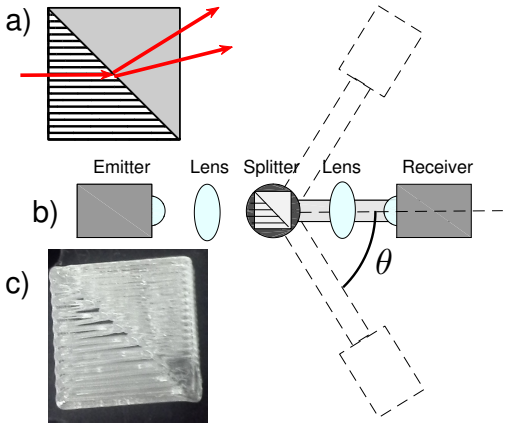

Fig. 3 a) Schematic representation of the proposed structure indicating where the separation of polarizations occur. b) Experimental setup. One half of the system was fixed on the table while the other half was mounted on a rotatory stage in order to take measurements at angles ranging from $-90°$ to $90°$, being $0°$ the straight position through the emitter, in order to detect the deflected radiation by the device which remained fixed in the center. c) Picture of the fabricated device.

two polarizations at 100 GHz are shown in Fig. 2a and b respectively. The colourmaps show that the radiation is refracted at the 45° interface at considerably different angles remaining relatively collimated after propagating through the entire structure. Similar simulations are presented in Fig. 2c and d for 600 GHz. In this case the beams for the two polarizations are still deflected at different angles, but the radiation does not remain collimated and a more complex diffraction structure appears. The deflected angles are 29° and 11° for the polarization parallel and perpendicular respectively

In order to test our device, we used a Menlo system Tera K15 fiber coupled spectrometer in transmission configuration. The radiation was produced in an InGaAs photoconductive emitter, and two TPX lenses were used to collimate and focus the radiation on the sample. Two additional TPX lenses and an InGaAs photoconductive detector were mounted on a mobile arm driven by a computer controlled rotational stage in order to measure terahertz waveforms as function of the angle as shown in Fig. 3 b.

The device was fabricated by 3D printing with Bendlay (n=1.53 below 1 THz). The device is a cubic structure of 2 cm side with a layered structure in one half and a solid material in the other The two halves meet at a 45° angle with respect to the cube walls. In order to test the device it was mounted at the sample position and remained fixed. Waveforms were recorded for angles between $-90°$ and $90°$ in $1°$ steps, where $0°$ corresponds to the optical axis in the absence of the prism. The emitter and detector were first placed so that the radiation was produced and detected with polarization perpendicular to

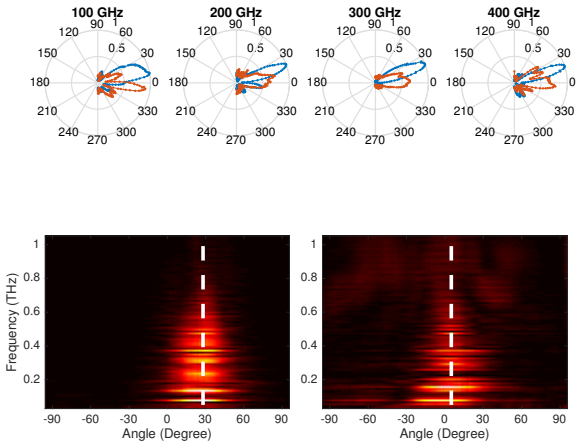

Fig. 4 Radiation patterns at different frequencies after propagation through the device. Dotted lines are radiation with polarization parallel to the structure layers and solid lines are radiation with polarization perpendicular to the layers. For frequencies between 200 GHz and 300 GHz the radiation is well separated for the two polarizations and it remains reasonably well collimated. For 100 GHz and 400 GHz the radiation was spread or overlapping. At the 100 GHz the signal to noise ratio in the spectrometer was poor but polarization separation remains. At 400 GHz the features of the structure are in the order of the wavelength. e) and f) are the deflected angle at every frequencies for polarization perpendicular to the material layers and parallel to the material layers respectively. The discontinuos lines are lines at 28° and 5° as a guide to the eye.

the layered structure, and subsequently the experiment was repeated with the emitter and detector rotated so that radiation had polarization parallel to the layered structure.

After acquiring the data sets for the two polarizations, each waveform was Fourier transformed. The radiation patterns for the polarization parallel (continuous) and perpendicular (dashed) to the birefringent structure walls as a function of the angle are shown in the polar plots in Fig. 4a, b, c and d for 100 GHz, 200 GHz, 300 GHz and 400 GHz respectively. These plots show that the radiation polarized perpendicular to the structure was deflected about 30°, while the one parallel was deflected about 0°. The 100 GHz and 400 GHz plots show a complex structure of the patterns, being poor signal-to-noise ratio and diffraction the reasons respectively. In order to have a better picture, the angle and frequency dependent amplitude of the two polarizations are shown as colormaps in Fig. 4e and f. These plots confirm that the radiation is deflected at around 28° and 0° all across the spectrum and that additional diffracted "orders" with smaller amplitude appear at angles larger than 50° at frequencies higher than 400 GHz. The discontinuos lines are lines at 28° and 5° as a guide to the eye.

The device showed an electric field amplitude (power) cross polarization extinction ratio of 0.02 (4×10^{-4}) and 0.04 (1.6×10^{-3}) for the parallel and per-

pendicular components respectively at 200 GHz. In addition the transmittance for the parallel and perpendicular components were 0.23 and 0.24 respectively also at 200 GHz.

In this letter we report the design, fabrication and characterization of a 3D printed terahertz polarization splitter based on form birrefringence, similar to a Wollaston prism. The structure consist in a 2 cm side cube made of Bendlay (n=1.53 below 1 THz). One half of the device consists of a birrefringent triangular structure and the other half is a solid prism. The device operates very well for frequencies below 400 GHz. The device showed a cross polarization extinction ratio better than 1.6×10^{-3} and a transmission better than 0.23. A polarization splitter such as this one is useful for the construction of terahertz photonic systems and might be applied to multiplexing and demultiplexing signals for terahertz telecommunications. In addition, the mass production of this component is viable, either by 3D printing or by the use of an appropriate mold at very reasonable costs. Furthermore we confirm that 3D printing is promising technique for prototyping and fabricating relatively sophisticated quasi-optical devices, currently unavailable, for terahertz frequencies.

Acknowledgements

The authors would like to acknowledge the financial support from Consejo Nacional de Ciencia y Tecnologia (grant numbers 255114 and 252939). A. I. Hernandez-Serrano would like to acknowledge a scholarship from Consejo Nacional de Ciencia y Tecnologia (354621).

References

1. S. Ergün, S. Sönmez, Journal of Military and Information Science **3**(1), 13 (2015)
2. R.I. Stantchev, B. Sun, S.M. Hornett, P.A. Hobson, G.M. Gibson, M.J. Padgett, E. Hendry, Science Advances **2**(6), e1600190 (2016)
3. J.F. Federici, B. Schulkin, F. Huang, D. Gary, R. Barat, F. Oliveira, D. Zimdars, Semiconductor Science and Technology **20**(7), S266 (2005)
4. A. Hernandez-Serrano, S. Corzo-Garcia, E. Garcia-Sanchez, M. Alfaro, E. Castro-Camus, Applied Optics **53**(33), 7872 (2014)
5. M. Stecher, C. Jördens, N. Krumbholz, C. Jansen, M. Scheller, R. Wilk, O. Peters, B. Scherger, B. Ewers, M. Koch, in *Ultrashort Pulse Laser Technology* (Springer, 2016), pp. 311–335
6. M. Theuer, R. Beigang, D. Grischkowsky, Applied Physics Letters **97**(7), 071106 (2010)
7. K. Fukunaga. Thz technology applied to cultural heritage in practice, (Springer, Japan, 2016), pp.1–144
8. C.L. Koch-Dandolo, T. Filtenborg, K. Fukunaga, J. Skou-Hansen, P.U. Jepsen, Applied Optics **54**(16), 5123 (2015)
9. W. Hu, S. Catalano, M. Gibert, J.M. Triscone, A. Cavalleri, Physical Review B **93**(16), 161107 (2016)
10. N. Oshima, K. Hashimoto, D. Horikawa, S. Suzuki, M. Asada, in *2016 IEEE MTT-S International Microwave Symposium (IMS)* (IEEE, 2016), pp. 1–4
11. C. Han, A.O. Bicen, I.F. Akyildiz, IEEE Transactions on Signal Processing **64**(4), 910 (2016)

12. H.J. Song, K. Ajito, Y. Muramoto, A. Wakatsuki, T. Nagatsuma, N. Kukutsu, Electronics Letters **48**(15), 953 (2012)
13. S. Busch, M. Weidenbach, M. Fey, F. Schäfer, T. Probst, M. Koch, Journal of Infrared, Millimeter, and Terahertz Waves **35**(12), 993 (2014)
14. Squires, A. D., E. Constable, R. A. Lewis. Journal of Infrared, Millimeter, and Terahertz Waves **36**(1) 72-80 (2015).
15. S. Busch, M. Weidenbach, J. Balzer, M. Koch, Journal Infrared, Millimeter, Terahertz Waves **37**, 303-307 (2015)
16. A. Hernandez-Serrano, M. Weidenbach, S. Busch, M. Koch, E. Castro-Camus, Journal of the Optical Society of America B **33**(5), 928 (2016)
17. K. Nielsen, H.K. Rasmussen, A.J. Adam, P.C. Planken, O. Bang, P.U. Jepsen, Optics Express **17**(10), 8592 (2009)
18. J. Fan, Y. Li, M. Hu, L. Chai, C. Wang, IEEE Photonics Technology Letters **28**(10), 1096 (2016)
19. J. Liu, R. Mendis, D.M. Mittleman, Applied Physics Letters **103**(3), 031104 (2013)
20. D. Headland, W. Withayachumnankul, M. Webb, H. Ebendorff-Heidepriem, A. Luiten, D. Abbott, arXiv preprint arXiv:1605.03246 (2016)
21. S. Pandey, B. Gupta, A. Nahata, Optics Express **21**(21), 24422 (2013)
22. Vogt, Dominik Walter, Rainer Leonhardt, Journal of Infrared, Millimeter, and Terahertz Waves **37**(11) 1086-1095 (2016)
23. Vogt, Dominik Walter, Jessienta Anthony, Rainer Leonhardt, Optics Express **23**(26), 33359-33369 (2015).
24. Yudasari, Nurfina, Jessienta Anthony, and Rainer Leonhardt, Optics Express **22**(21), 26042-26054 (2014).
25. M. Scheller, C. Jördens, M. Koch, Optics Express **18**(10), 10137 (2010)
26. C. Larsen, D.G. Cooke, P.U. Jepsen, Journal of the Optical Society of America B **28**(5), 1308 (2011)